

Neural Radiance and Gaze Fields for Visual Attention Modeling in 3D Environments

Andrei Chubarau, Yinan Wang, James J. Clark
McGill University
Centre for Intelligent Machines

{andrei.chubarau@mail, yinan.wang2@mail, james.clark1@}.mcgill.ca

Abstract

We introduce *Neural Radiance and Gaze Fields (NeRGs)* as a novel approach for representing visual attention patterns in 3D scenes. Our system renders a 2D view of a 3D scene with a pre-trained *Neural Radiance Field (NeRF)* and visualizes the gaze field for arbitrary observer positions, which may be decoupled from the render camera perspective. We achieve this by augmenting a standard NeRF with an additional neural network that models the gaze probability distribution. The output of a NeRG is a rendered image of the scene viewed from the camera perspective and a pixel-wise saliency map representing conditional probability that an observer fixates on a given surface within the 3D scene as visible in the rendered image. Much like how NeRFs perform novel view synthesis, NeRGs enable the reconstruction of gaze patterns from arbitrary perspectives within complex 3D scenes. To ensure consistent gaze reconstructions, we constrain gaze prediction on the 3D structure of the scene and model gaze occlusion due to intervening surfaces when the observer’s viewpoint is decoupled from the rendering camera. For training, we leverage ground truth head pose data from skeleton tracking data or predictions from 2D saliency models. We demonstrate the effectiveness of NeRGs in a real-world convenience store setting, where head pose tracking data is available.

1. Introduction

Predicting human attention in 3D environments is an important yet under-explored research area. Visual attention is typically represented as the probability of fixation of viewers on various visual stimuli. Prior research on attention prediction primarily focuses on 2D attention, i.e., image saliency for static 2D images [18, 26, 27, 30, 36], or gaze estimation from the egocentric perspective [31, 35, 54, 61]. The context in which visual attention is measured often has a strong effect on the gaze patterns: observers show dif-

ferent attention patterns when performing different tasks [40, 47]. In a free-viewing setting, gaze patterns are more spontaneous and exploratory, while task-specific settings may guide observers towards certain objects or patterns.

While prior work mainly focuses on modeling attention in 2D images, we explore models that predict and visualize attention patterns for 3D environments. There are two main considerations for representing visual attention in 3D: (i) a way of representing the 3D geometry of a scene, such as the shape and position of objects, and (ii) a method for acquiring, representing, and mapping visual attention data relative to the objects and surfaces in a 3D scene.

As 3D objects are typically represented using meshes, various *mesh saliency* techniques [32, 33, 39, 48] have been developed to predict eye fixation densities directly on 3D surfaces, both for individual objects and composite scenes. However, these methods are computationally expensive and require existing meshes, limiting their application when mesh data is unavailable. Reconstructing meshes from 2D images remains challenging [55], while manually modeling meshes is a tedious and time-consuming process [5], especially for detailed objects and surfaces.

Neural Radiance Fields (NeRFs) [42] offer a compelling alternative for modeling 3D environments. NeRFs enable novel view synthesis, allowing the reconstruction of 3D scenes from arbitrary perspectives. Unlike traditional mesh-based approaches, which require labor-intensive modeling and texturing, NeRFs produce high-quality 3D representations in just a few minutes given a set of 2D views of a 3D scene as input [43]. This capability makes NeRFs particularly well-suited for 3D applications where meshes are unavailable or impractical to create.

In this work, we leverage NeRFs to model visual attention in complex 3D scenes. We frame gaze visualization as a rendering problem: similar to how NeRFs model spatial color and density, we model spatial gaze. In our setting, we use the term “gaze” to refer to the ground-truth data used to train NeRG, which may be derived from saliency maps, eye fixations, head-pose tracking, and other sources.

Our method effectively learns to map such gaze signals to surfaces within the implicit 3D environment encoded by a pre-trained NeRF, which we can then reconstruct from arbitrary camera perspectives. Unlike most prior work, we account for gaze occlusion by decoupling the observer and rendering camera perspectives: surfaces visible to the rendering camera may be occluded from the observer, preventing direct gaze. Finally, our method remains lightweight by building on top of efficient NeRF implementations [43].

Our main contributions are as follows:

- We propose Neural Radiance and Gaze Fields (NeRGs), which extend the standard NeRFs with a gaze prediction network constrained on the 3D geometry of the scene, enabling implicit mapping between human visual attention and complex 3D environments.
- Our method reconstructs gaze patterns for arbitrary observer and rendering camera perspectives: unlike prior work, we decouple the observer view (gaze ray) and the rendering camera view (volume rendering ray) allowing our model to consider gaze occlusion within the 3D scene.
- We evaluate NeRGs in a case study using authentic gaze tracking data. With NeRG, we can synthesize novel views of the 3D scene and efficiently visualize 3D attention patterns for customizable observer positions.

2. Related Work

2.1. Visual Saliency

Visual saliency is typically quantified and visualized using saliency maps that highlight regions of an image likely to attract attention [6]. Early computational models of visual saliency focused on analyzing fundamental image features such as intensity patterns, color, and edge orientation [18, 23], employing various strategies to refine and extract relevant information [1, 15, 21, 59, 60]. More recently, deep learning has become central to visual saliency prediction [25, 28, 29, 34, 37, 52]. To capture the complex dynamics of human visual attention, neural networks are trained on eye-tracking data from both free-viewing and task-specific settings [7, 19]. A prominent example is the DeepGaze family of models [26, 27, 30], which leverage deep features from pre-trained convolutional neural networks to predict saliency or eye fixation positions in 2D images.

2.2. Saliency in 3D

Prior work on eye tracking [24, 38, 57] and gaze target prediction from third-person videos [10, 11, 22, 45] primarily focuses on 2D image analysis, which is notably different from saliency in 3D environments. A line of work explores projection of 2D saliency onto 3D scenes [32, 41], while others directly model mesh saliency to describe attention over 3D objects [33, 39, 48]. However, recent research suggests that saliency in complex 3D environments cannot be

fully explained by 2D methods [12, 49, 53, 56]. Studies of attention in virtual environments and virtual reality (VR) further highlight the relationship between head movement and gaze behavior. Specifically, fixations tend to occur at low head velocities, suggesting that 3D saliency can be inferred from the observer’s head orientation even in the absence of gaze tracking [14].

2.3. Egocentric Gaze Estimation

Egocentric gaze estimation methods model attention from the perspective of an observer [31, 50, 61], where videos from the first-person perspective are used to track gaze patterns [16, 17, 44, 51]. A common challenge in egocentric gaze estimation, however, stems from poor temporal consistency of the fixation data due to high varying gaze patterns between video frames.

2.4. Neural Radiance Fields

Neural Radiance Fields (NeRFs) reconstruct 3D scenes by mapping 2D image data to a continuous volumetric function. For a given position (x, y, z) and viewing direction (θ, ϕ) , NeRFs evaluate volume density σ and a view-dependent RGB color associated with the given query. Images are synthesized via volume rendering where density and color samples are integrated along a camera ray to compute pixel values in the rendered image. NeRFs are trained to generate images that closely resemble the training data by minimizing perceptual difference between rendered views and the ground-truth images. Recent advancements in NeRF algorithms have significantly enhanced both rendering speed and quality [2–4, 43], enabling more accurate and efficient 3D scene representation. These improvements also introduce greater flexibility, for instance the ability to edit trained NeRFs [58].

3. Preliminaries

We consider the task of rendering gaze patterns in a 3D environment given by a pre-trained NeRF. Specifically, our goal is to evaluate gaze for different observers within the 3D

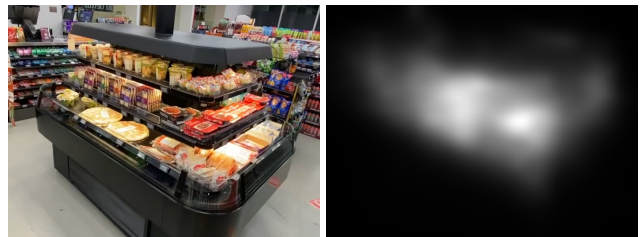


Figure 1. Visualizing 2D saliency for a 3D scene. (Left) A view of a 3D scene rendered by evaluating a pre-trained NeRF. (Right) Probability density of gaze predicted by DeepGaze IIe [36], a standard 2D saliency model.

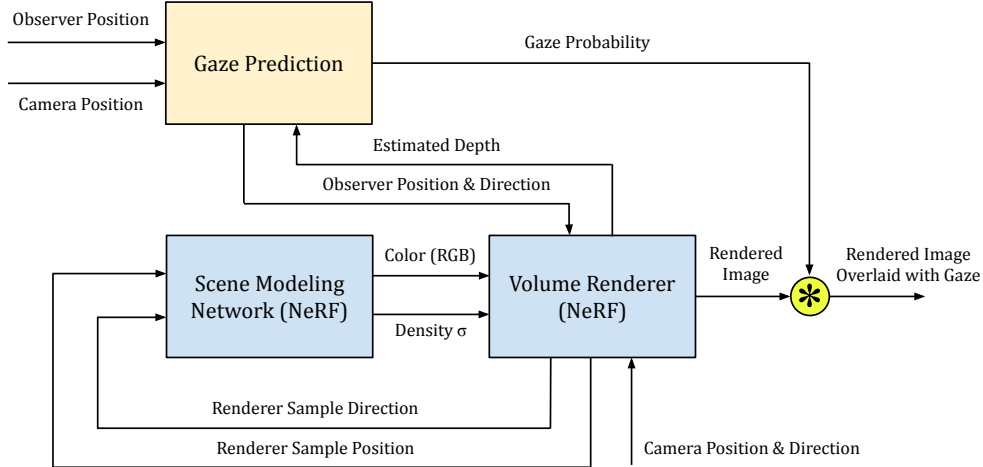


Figure 2. Overall system diagram of the Neural Radiance and Gaze Field (NeRG). We evaluate a NeRF with volume rendering and visualize gaze for the visible surfaces. Gaze is predicted from the observer’s perspective, which can be decoupled from the rendering camera.

world visualized by 2D images rendered with NeRF. Some parts of the rendered scene, although visible from the rendering camera perspective, may be occluded when viewed from a distinct observer perspective. Handling gaze occlusion is therefore a critical component in our work.

The simplest way to extend NeRFs with gaze is to apply a standard 2D saliency model such as DeepGaze [27] to the 2D renders of the scene. We demonstrate this straightforward approach in Figure 1, showcasing the 2D saliency map predicted by DeepGaze IIe [36] for a given rendered view. However, standard deep 2D saliency prediction models have notable limitations when used alongside NeRFs. To begin, the use of complex 2D saliency networks implies significant computational overhead. Every rendered frame must be processed by a large 2D saliency network, which can be prohibitive for real-time applications. Such models may also produce inconsistent predictions when applied to images rendered by NeRF due to its intrinsic rendering artifacts (floaters, etc.) or camera movement. Moreover, 2D saliency methods require 2D image inputs and therefore do not consider the underlying 3D geometry of the world. While one could map 2D saliency onto the 3D scene, e.g., by 3D projections of depth, this requires that the rendering camera and observer perspectives be aligned, restricting observer position to the camera position.

4. Neural Radiance and Gaze Fields

We present Neural Radiance and Gaze Fields (NeRGs), a novel method for representing and visualizing gaze in 3D environments. Our approach extends Neural Radiance Fields (NeRFs) by integrating a gaze prediction module as illustrated in Figure 2. Specifically, we constrain gaze prediction on the 3D geometry of the rendered scene encoded

by a pre-trained NeRF. For a given pixel, we first evaluate the NeRF from position \mathbf{p} along ray direction \mathbf{r} to obtain the corresponding pixel color with volume rendering. We use the depth d along the traced ray to compute the position of the visible surface $\mathbf{p}_d = \mathbf{p} + d\mathbf{r}$. While NeRFs do not explicitly model depth, a coarse estimate of depth can be recovered by accumulating density values during the volume rendering process [42]. We compute gaze by evaluating a lightweight network for a “gaze ray” defined from the specified observer position \mathbf{p}_o towards the surface located at \mathbf{p}_d , which we illustrate graphically in Figure 3.

Unlike prior methods, our system allows the position of the observer and the rendering camera to be decoupled, enabling visualization of gaze with more flexibility and finer user control. When the observer is decoupled, surfaces visible from camera perspective may appear occluded for an observer. NeRG handles gaze occlusion by testing depth from the observer’s perspective: a discrepancy between the expected and evaluated depth values implies occlusion along the gaze ray.

4.1. Modeling 3D Gaze

To render gaze patterns on 3D surfaces, we model gaze as a signal that originates at the surface of 3D objects and is perceived by an external observer. In this setting, surfaces “emit” attention, while observers “capture” the emitted signal. This formulation of gaze has two important properties. First, it constrains gaze prediction on the 3D geometry of the scene by explicitly incorporating the positional information of the visible surface as seen from the observer’s perspective. We find that this is a required property to ensure consistent reconstructions of gaze patterns from arbitrary viewpoints unseen during training. Second, gaze predictions are also conditioned on the observer’s position,

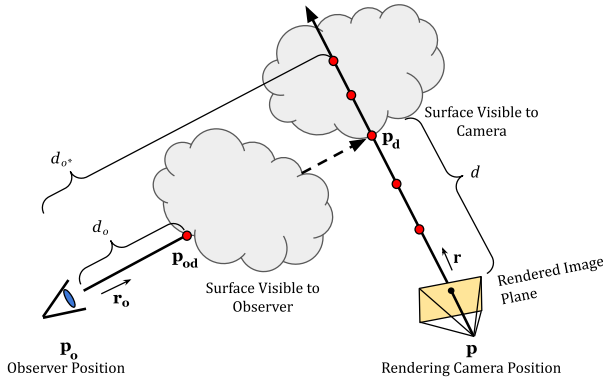


Figure 3. Gaze prediction in NeRG. Volume rendering of the NeRF produces a depth estimate along the traced ray. Gaze is evaluated between the position of the visible surface and the position of the observer. If the observer is decoupled from the rendering camera, gaze occlusion can be modeled by additionally evaluating depth from the observer’s perspective to correct the position of the surface visible to the observer.

which we can decouple from the rendering camera perspective, allowing the system to visualize gaze patterns with greater flexibility. We can additionally model gaze occlusion by testing visibility from the observer’s perspective, which is facilitated by using a NeRF to represent scene geometry. Similarly to how objects cast shadows to occlude light, emitted gaze can be occluded from an observer.

4.2. Gaze Prediction Module

Following NeRF, we approximate a continuous spatial function parameterized by an MLP neural network $F_{\Theta} : (\mathbf{p}, \mathbf{r}) \rightarrow g$ for input position $\mathbf{p} = (x, y, z)$ and ray direction $\mathbf{r} = (\theta, \phi)$. Instead of density and color (as in NeRF), our model encodes a directional gaze signal g . To model emitted and captured gaze, we further define two identical networks, F_e and F_c . The network F_e encodes the directional gaze signal emitted from position \mathbf{p}_{od} (surface visible to observer). The network F_c models the capturing of gaze at position \mathbf{p}_o (observer position). Gaze prediction is then defined as follows:

$$G(\mathbf{p}_{od}, \mathbf{p}_o) = F_e(\mathbf{p}_{od}, -\mathbf{r}_o) \times \text{sigmoid}(F_c(\mathbf{p}_o, \mathbf{r}_o)), \quad (1)$$

where \mathbf{r}_o describes the direction from \mathbf{p}_o to \mathbf{p}_{od} . We apply a sigmoid function to the output of F_c to ensure that an observer cannot capture more gaze signal than is emitted. Fundamentally, our formulation conditions predicted gaze on the positions of the visible surface and the observer, i.e., $G(\mathbf{p}_{od}, \mathbf{p}_o)$ can model the conditional probability of gaze $\Pr(G = g | \mathbf{p}_{od}, \mathbf{p}_o)$. In this setup, gaze capturing is necessary to model spatial variations in gaze patterns along a vector from a given surface—the emission component alone

cannot achieve this, as emitted gaze remains constant along a given direction (similar to radiance).

In practice, the networks F_e and F_c share most of the network weights, embedding input position and direction into a shared latent space. However, each network has a distinct final fully connected layer that processes the extracted geometric features to compute its respective output.

By applying Equation 1, we do not need to accumulate gaze along a ray, as done for density and color in NeRF. This is intentional to ensure reduced computational overhead. However, we must evaluate a pre-trained NeRF to obtain depth from the observer’s perspective. This step can be done efficiently by evaluating only the density component of NeRF, since we do not use the color. Moreover, in this training setup, the observer and rendering camera perspectives (used to evaluate depth) are aligned; gaze occlusion therefore does not need to be handled. Lastly, a mapping between the gaze data and the NeRF coordinate system must be known to enable depth testing with a NeRF.

4.3. Handling Gaze Occlusion

When the observer and rendering camera perspectives are decoupled, gaze occlusion by intervening surfaces needs to be handled. We test for gaze occlusion by evaluating depth from the observer perspective and comparing it to the expected depth. We evaluate observer depth with an additional volume rendering pass by the NeRF (only its density). As illustrated in Figure 3, depth d is measured from the rendering camera position, depth d_o is the evaluated depth from the observer perspective, and d_{o*} is the expected depth given by $\|\mathbf{p}_o - \mathbf{p}_d\|$.

When $d_o < d_{o*}$, the surface visible to the camera is occluded from the perspective of the observer, which implies gaze occlusion. This comparison acts as a binary indicator of visibility from the observer. For a smoother transition, we define the gaze shadowing factor s with a fall-off parameter d_f , namely $s = (d_{o*} - d_o) / d_f$. A larger fall-off value produces a gaze penumbra effect which is visually preferred to the sharp and high variance shadowing resulting from a boolean comparison. We finalize by multiplying gaze probability by the gaze shadowing factor. Note that we also clamp s such that $0.0 < s < 1.0$.

Although the depth evaluated by NeRFs may have high variance, even in areas where it is expected to be roughly constant, we find that this test is sufficient to model visibility in the encoded 3D environment.

4.4. Loss Functions

We train NeRG to predict a ground-truth signal related to gaze. Given the ground-truth and predicted values, \mathbf{y} and $\hat{\mathbf{y}}$, respectively, we optimize the loss functions commonly used in saliency prediction [8, 29, 37], namely linear correlation coefficient (CC), Kullback-Leibler Divergence (KLD), and

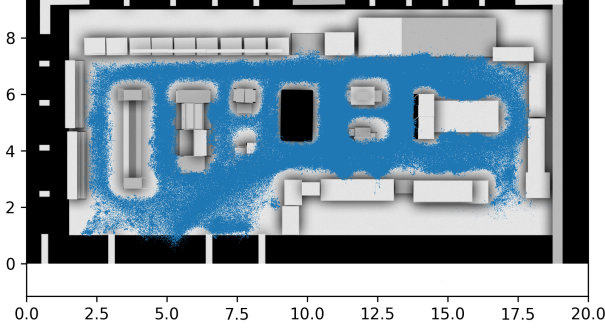


Figure 4. The layout and dimensions of the convenience store (in meters). Blue point cloud illustrates individual gaze rays from the available pose tracking data. Data from [54].

optionally Mean Average Error (MAE), which are defined as follows:

$$L_{CC}(\mathbf{y}, \hat{\mathbf{y}}) = \frac{\text{cov}(\mathbf{y}, \hat{\mathbf{y}})}{\sigma(\mathbf{y})\sigma(\hat{\mathbf{y}})}, \quad (2)$$

where $\text{cov}(\cdot)$ is covariance and $\sigma(\cdot)$ is standard deviation;

$$L_{KLD}(\mathbf{y}, \hat{\mathbf{y}}) = \sum_{i=1}^N \mathbf{y}_i \log \left(\frac{\mathbf{y}_i}{\hat{\mathbf{y}}_i} \right), \quad (3)$$

where N represents the number of samples;

$$L_{MAE}(\mathbf{y}, \hat{\mathbf{y}}) = \frac{1}{N} \sum_{i=1}^N |y_i - \hat{y}_i|. \quad (4)$$

We optimize the sum of the individual loss functions.

5. Case Study: Application of NeRG

A growing number of retail outlets employ systems that track the movement of customers within their premises (e.g., C2RO’s ENTERA [9]). This motivates a qualitative study of NeRG where we apply our system to an extensive skeleton tracking dataset of shoppers in a convenience store based on data by Wang et al. [54]. In addition to modeling eye gaze direction probabilities, the NeRG paradigm can be used to model any viewer-centered directional quantity, such as head pose and body pose. In our case study, we apply NeRG to model head pose, which is a sufficient proxy of gaze [14]. Johnson and Cuijpers [20], for instance, showed in an empirical study that head pose and eye gaze direction are almost linearly related. We make the simple assumption that eye gaze follows the direction of the head pose, and we loosely refer to the head pose as the gaze direction in what follows. Customers in the convenience store are tracked as skeleton data with 22 tracked points on the human body, termed *keypoints*. We use the left ear, right ear, and nose keypoints to compute head pose to model gaze direction.

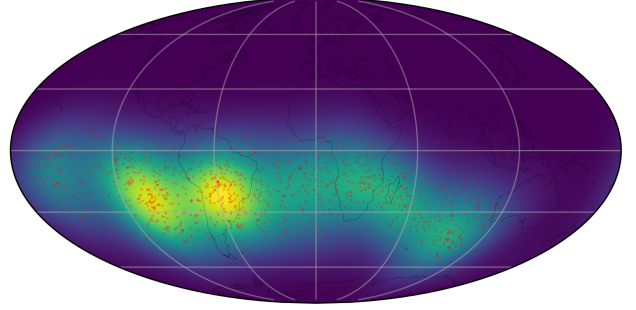


Figure 5. Gaze probability density over a sphere (Mollweide projection) for a randomly sampled gaze probe. Probability shown as heatmap, individual gaze rays forming the probe as red dots.

Training a NeRG requires a set of ground-truth samples describing gaze from different observer viewpoints within an environment modeled by a NeRF. Our system therefore relies on both gaze data and a sufficient number of views of the scene to enable training of a high-quality NeRF model.

First, we train the NeRF separately from the gaze prediction module by following the standard training procedure [42]. We then extend this with a NeRG by training our system on a set of gaze ray samples acquired with the process based on gaze probes outlined in subsection 5.1. We use a subset of the available tracking data corresponding to one day of shopping. We further spatially constrain the environment and consider a central area of the convenience store which is roughly aligned with the views of the store used to train a NeRF. The store environment is depicted in Figure 4.

In implementing NeRG, we build on top of a public PyTorch [46] repository of NeRF based on instant neural primitives [43] for efficient training and rendering¹. We release our code at <https://github.com/ch-andrei/nerg-neural-gaze>.

5.1. Training Data

We identify two strategies to obtain ground-truth training data for NeRGs: (i) we can leverage data from skeleton pose-tracking systems (head pose is sufficient to describe gaze [14]), and (ii) we can use existing 2D saliency models to generate gaze probabilities for static images (possibly rendered with NeRF). While our NeRG system can be extended to option (ii), our experiments mainly focus on option (i) due to the availability of skeleton-based gaze tracking data and the limitations of 2D saliency methods when applied to 3D scenes.

Gaze tracking data typically represents eye fixations or head pose with individual rays. We begin by processing individual rays to build a representation that can be used to train NeRGs. We construct a k -dimensional (k -d) tree for

¹<https://github.com/ashawkey/torch-ngp>

efficient data indexing into the dataset of gaze rays and cluster the individual rays into “gaze probes” within the considered 3D environment. A gaze probe is akin to probes in computer graphics, describing a 360° ego-centric gaze probability distribution at a given position. We acquire all gaze rays within a physical radius R of a given position and approximate the gaze probability distribution with kernel density estimation (KDE) over a sphere, using a Von-Misses Fisher spherical distribution [13] as the kernel. Note that the cumulative density function (CDF) of a gaze probe is equal to one. In a practical implementation, we limit the maximum number of gaze rays per gaze probe to 1024 to reduce the computational burden associated with KDE.

To train the NeRG, we generate a set of gaze probes from the available ray data. The probability density of one such gaze probe is illustrated in Figure 5. Gaze probes can be positioned uniformly on a 3D grid or their positions can be randomized. It is practical to precompute a set of gaze probes and repeat it every training epoch, because active indexing into a large dataset of rays can be time-consuming, even with a k-d tree. For each gaze probe, we evaluate a number of gaze rays to generate samples used to train our gaze prediction network. Gaze ray directions are sampled uniformly over the sphere. Our training data therefore consists of a set of gaze ray samples of the form $S : \{x, y, z, \theta, \phi, g\}$, representing sample position (given by gaze probe position), direction, and the associated gaze signal g , which is computed from the probability distribution modeled by KDE. This setup follows the format for predicting colors with NeRFs, except that we provide gaze probability instead of colors.

At each epoch, our system is trained to predict gaze for gaze rays obtained by sampling the generated gaze probes. A batch can contain gaze rays from individual gaze probes. Batch size then controls the number of sampled gaze rays per probe. The network is trained until convergence is achieved as indicated by monitoring the loss functions.

5.2. Aligning NeRF and Gaze Data

Trained NeRFs encode 3D scenes in an internal coordinate system distinct from the physical-world coordinates defined by pose-tracking systems. To enable gaze prediction within the NeRF-encoded space, gaze data must be aligned to the NeRF coordinate system. This alignment can be achieved by defining a transformation matrix between NeRF and world coordinates. In general, it is challenging to automatically determine the mapping between NeRF and world-space coordinates. We leverage the existence of a 3D digital twin of the convenience store, which we can visualize in 3D modeling software such as Blender® [5]. We first recover a coarse 3D mesh of the objects encoded by the NeRF by applying the marching cubes algorithm [43]. This recovered mesh is expressed in the NeRF coordinate system. To find

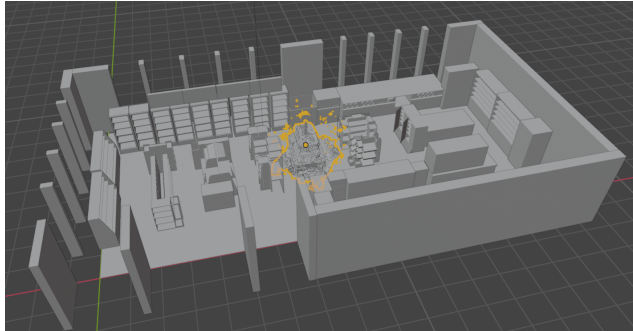


Figure 6. Alignment of the NeRF mesh with the 3D model of the convenience store in 3D modeling software. This step is necessary to acquire the transformation matrix between the NeRF coordinate system inherited in NeRG to represent the 3D scene, and the world coordinate system in which the pose-tracking data is collected.

the transformation matrix between the NeRF and gaze coordinates, we manually align the mesh from NeRF to the digital twin model of the physical store in 3D modeling software, as depicted in Figure 6. The world transformation matrix M_w of the aligned mesh corresponds to the transformation between NeRF and gaze data. Given a homogeneous coordinate $[x, y, z, 1]$ in the NeRF coordinate system, we can pre-multiply this coordinate by the transformation matrix M_w to get the corresponding homogeneous coordinate in the world coordinate system. Similarly, the inverse of this matrix maps from gaze data to NeRF coordinates.

5.3. Visualizing Gaze with NeRG

We illustrate gaze heatmaps predicted by a trained NeRG model in Figure 7, comparing predictions by NeRG to the ground-truth encoded by our gaze probes at the given positions. We further demonstrate the decoupling of the observer’s position from the rendering camera position in Figure 8. NeRG handles gaze occlusion by modulating gaze patterns by the visibility of surfaces from the observer’s perspective. Figure 8 highlights how the object’s geometry occludes gaze rays, preventing an observer from attending to a surface visible in the rendered view.

5.4. Evaluations and Ablations

We evaluate NeRG on views unseen during training, comparing the expected and the predicted gaze patterns. We use the loss functions defined in subsection 4.4 as the evaluation criteria to compare our models. Ultimately, we find that following the network architecture and hyperparameters standard to NeRFs leads to our best results, namely we configure NeRG with identical network size, hidden dimension, etc. as the used NeRF model. While we explored various network designs and complexities through ablations, the default configuration remained the most effective.

However, our tests highlight the importance of the gaze

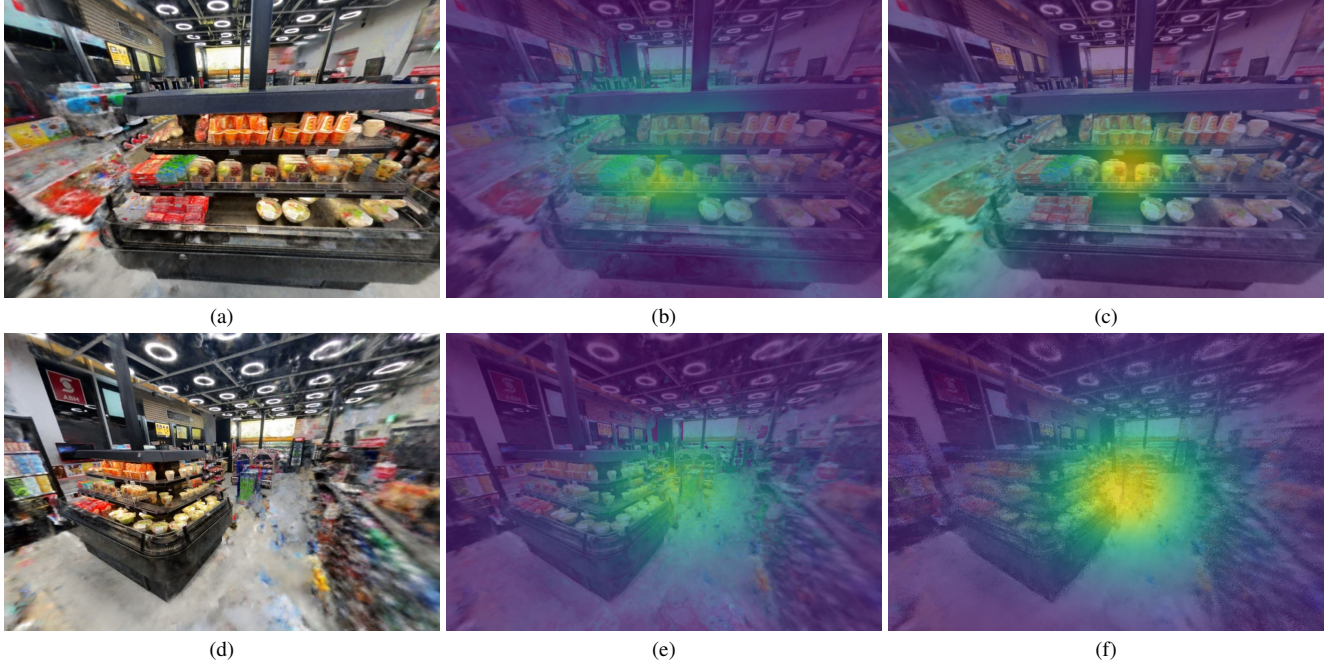


Figure 7. Gaze visualized by NeRG and gaze probes from different view perspectives. The rendered scene is shown in (a) and (d); gaze predictions (overlay) by a trained NeRG in (b) and (e); ground-truth gaze by gaze probes in (c) and (f). Gaze probes represent gaze by applying KDE over local gaze rays given our gaze data, which may be noisy, spatially inconsistent, and slow to compute (over 5 seconds to evaluate a frame at 720p). NeRG learns spatially consistent gaze patterns while rendering at interactive framerates (less than 100ms).

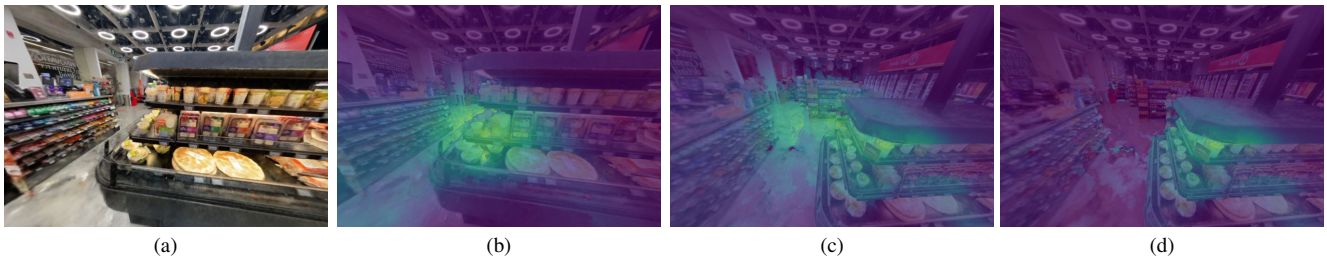


Figure 8. The effect of gaze occlusion for decoupled observer and rendering camera perspectives. (a) scene rendered from the observer’s position; (b) gaze predictions by a trained NeRG; (c) observer is in (a), but rendering camera is moved left and up; (d) same as (c) but accounting for gaze occlusion. Notice that in (d) gaze is occluded for surfaces behind the shelf which are not visible to the observer.

emit-capture model introduced in subsection 4.1 and defined by Equation 1, as it is critical for reconstructing spatially consistent gaze patterns. In our experiments, we find that networks trained to predict gaze directly from the observer’s perspective—without conditioning on the position of the visible surface—fail to generalize effectively.

6. Discussion

6.1. Comparison to Saliency Mapping Methods

Our method has multiple advantages over existing techniques for 3D attention. First, NeRG inherits the understanding of 3D geometry intrinsic to NeRFs. Because we employ a pre-trained NeRF to represent the 3D environ-

ment, NeRG does not require complex additional models for depth estimation or 3D mapping of 2D saliency. While many prior methods project 2D saliency onto 3D scenes, gaze prediction in NeRG follows the design of NeRF-like systems and directly evaluates a probability of gaze in 3D given an observer position and a gaze ray direction.

In addition, since we employ a lightweight fully-connected neural network to predict gaze—similar to networks used in NeRFs—gaze prediction by NeRG is efficient. We can rapidly generate 2D views of the scene by evaluating NeRF from a given camera perspective, followed by gaze prediction for arbitrary observers located within the 3D scene. While the gaze prediction network must be evaluated for every pixel in the image rendered by NeRF, the

computational burden is significantly lighter than that required for a standard 2D image salience prediction network. Our method can further benefit from various optimizations from the recent work on NeRFs, suggesting that future improvements for NeRFs can likewise enhance NeRGs.

Our method also supports decoupled render camera and observer perspectives, allowing it to account for gaze occlusion. We formulate gaze from the observer’s perspective: gaze rays are defined between visible surfaces (from the render camera perspective) and the observer’s position. Conventional 2D salience methods cannot be applied for decoupled views because they require a 2D image as input, while it is challenging to synthesize a 2D view from a decoupled observer.

Lastly, although our current experiments focus on using gaze data from pose-tracking systems—such information is not commonly available for arbitrary 3D environments—we can easily extend NeRG to leverage 2D salience methods to generate training data. There are certain challenges with this modified version of NeRG but our early explorations offer promising results. We leave this to future work.

6.2. Limitations

Training and evaluating NeRGs. It is difficult to benchmark NeRG on existing 3D gaze data, because most gaze datasets are not designed for the training of NeRFs. In addition, these datasets commonly contain simple objects rather than complex 3D scenes where NeRGs excel. The alignment between gaze data and the NeRF-space coordinate system is also challenging. This step is, however, required to correctly represent gaze for rendered views of the scene. Training multiple NeRFs is also time consuming. Lastly, most prior salience methods do not consider both complex 3D environments and gaze occlusion. We therefore struggled to define a fair comparison against existing techniques. We leave such metrics and benchmarks to future work.

NeRF rendering artifacts. Since NeRG is built on top of NeRFs, our method inherits similar limitations to the original system. For example, NeRF rendering artifacts, such as floaters, may affect the rendered visualizations. If the NeRF network fails to reconstruct a high-quality view of the scene, NeRG may also produce a low-quality visualization. However, because we use a separate process and networks to model gaze, the predicted gaze patterns may have different visual artifacts or inaccuracies. That said, our method can benefit from any existing or future improvements that apply to NeRFs. Note that the emphasis of this work is not on the quality of NeRFs but rather on their application for gaze prediction.

Accuracy of depth estimation. NeRFs do not directly model depth, and the estimates of depth that we recover from volume rendering may be inaccurate. However, we use the estimated depth to model the positions of the visi-

ble surfaces, as well as to test visibility between two spatial locations. The low accuracy of depth estimates may lead to suboptimal gaze prediction and gaze occlusion.

Gaze occlusion. While gaze occlusion is useful in visualizing gaze patterns for arbitrary observers, authentic gaze data does not explicitly model this. Gaze tracking data naturally excludes gaze towards unseen surfaces: human observers simply do not pay attention to things that they cannot see. In NeRG, gaze occlusion is specifically relevant when the rendering camera and the observer perspectives are decoupled, which isn’t the case in the free viewing scenario. We therefore only evaluate the effect of gaze occlusion qualitatively.

Using head pose to model gaze. We assume that head poses describe the viewing direction and therefore gaze. While this assumption may be reasonable in some situations, e.g., large unstructured environments in natural outdoor settings, it may not hold true in structured environments like a store. For instance, head-tracking data from the convenience store may describe a person’s movement through the store and not necessarily their attention.

Using 2D salience to model gaze NeRGs can be trained on ground-truth gaze patterns predicted by 2D salience methods applied to views rendered by NeRF. However, 2D salience prediction algorithms may produce inaccurate salience maps in this particular application for two reasons. First, most state-of-the-art 2D salience prediction methods, such as DeepGaze IIe, are trained on data acquired during free-viewing, which may not be a valid assumption for our use case. Moreover, these models are trained on fixation data obtained while viewing 2D images, typically on a computer screen. Human attention is different in 3D environments, especially when observers perform specific tasks. For instance, in a convenience store, shoppers are frequently engaged in a search task, actively searching for products.

7. Conclusion

In this work, we presented Neural Radiance and Gaze Fields (NeRGs), a novel method for modeling and visualizing gaze patterns in complex 3D environments. By augmenting a pre-trained Neural Radiance Field (NeRF) with a gaze prediction module, NeRGs enable rendering of gaze patterns alongside scene reconstructions. Our approach supports gaze visualization from arbitrary observer viewpoints, optionally decoupled from the rendering camera, and considers gaze occlusion by 3D geometry to ensure spatially consistent gaze visualization. We demonstrate the effectiveness of NeRGs through experiments in a real-world convenience store setting, leveraging head pose data from skeleton tracking to train our system. Altogether, NeRGs enable real-time visualization of complex 3D-aware gaze patterns from arbitrary observer and rendering viewpoints, offering greater flexibility and user control in visualizing gaze.

References

- [1] Hossein Adeli, Françoise Vitu, and Gregory J Zelinsky. A model of the superior colliculus predicts fixation locations during scene viewing and visual search. *Journal of Neuroscience*, 37(6):1453–1467, 2017. 2
- [2] Jonathan T Barron, Ben Mildenhall, Matthew Tancik, Peter Hedman, Ricardo Martin-Brualla, and Pratul P Srinivasan. Mip-nerf: A multiscale representation for anti-aliasing neural radiance fields. In *Proceedings of the IEEE/CVF international conference on computer vision*, pages 5855–5864, 2021. 2
- [3] Jonathan T Barron, Ben Mildenhall, Dor Verbin, Pratul P Srinivasan, and Peter Hedman. Mip-nerf 360: Unbounded anti-aliased neural radiance fields. In *Proceedings of the IEEE/CVF conference on computer vision and pattern recognition*, pages 5470–5479, 2022.
- [4] Jonathan T Barron, Ben Mildenhall, Dor Verbin, Pratul P Srinivasan, and Peter Hedman. Zip-nerf: Anti-aliased grid-based neural radiance fields. In *Proceedings of the IEEE/CVF International Conference on Computer Vision*, pages 19697–19705, 2023. 2
- [5] Blender-Online-Community. *Blender - a 3D modelling and rendering package*. Blender Foundation, Stichting Blender Foundation, Amsterdam, 2018. 1, 6
- [6] G. T. Buswell. *How people look at pictures: a study of the psychology and perception in art*. Univ. Chicago Press, Oxford, England, 1935. Pages: 198. 2
- [7] Zoya Bylinskii, Tilke Judd, Ali Borji, Laurent Itti, Frédo Durand, Aude Oliva, and Antonio Torralba. MIT saliency benchmark. 2
- [8] Zoya Bylinskii, Tilke Judd, Aude Oliva, Antonio Torralba, and Frédo Durand. What Do Different Evaluation Metrics Tell Us About Saliency Models? . *IEEE Transactions on Pattern Analysis & Machine Intelligence*, 41(03):740–757, 2019. 4
- [9] C2RO. <https://www.c2ro.com/entera>. 5
- [10] Eunji Chong, Nataniel Ruiz, Yongxin Wang, Yun Zhang, Agata Rozga, and James M Rehg. Connecting gaze, scene, and attention: Generalized attention estimation via joint modeling of gaze and scene saliency. In *Proceedings of the European conference on computer vision (ECCV)*, pages 383–398, 2018. 2
- [11] Eunji Chong, Yongxin Wang, Nataniel Ruiz, and James M Rehg. Detecting attended visual targets in video. In *Proceedings of the IEEE/CVF conference on computer vision and pattern recognition*, pages 5396–5406, 2020. 2
- [12] Carlos Elmadjian, Pushkar Shukla, Antonio Diaz Tula, and Carlos H Morimoto. 3d gaze estimation in the scene volume with a head-mounted eye tracker. In *Proceedings of the Workshop on Communication by Gaze Interaction*, pages 1–9, 2018. 2
- [13] Ronald Fisher. Dispersion on a sphere. *Proceedings of the Royal Society of London. Series A, Mathematical and Physical Sciences*, 217(1130):295–305, 1953. 6
- [14] Tom Foulsham, Esther Walker, and Alan Kingstone. The where, what and when of gaze allocation in the lab and the natural environment. *Vision Research*, 51(17):1920–1931, 2011. 2, 5
- [15] Jonathan Harel, Christof Koch, and Pietro Perona. Graph-based visual saliency. *Advances in neural information processing systems*, 19, 2006. 2
- [16] Yifei Huang, Minjie Cai, Zhenqiang Li, and Yoichi Sato. Predicting gaze in egocentric video by learning task-dependent attention transition. In *Proceedings of the European conference on computer vision (ECCV)*, pages 754–769, 2018. 2
- [17] Yifei Huang, Minjie Cai, and Yoichi Sato. An ego-vision system for discovering human joint attention. *IEEE Transactions on Human-Machine Systems*, 50(4):306–316, 2020. 2
- [18] Laurent Itti, Christof Koch, and Ernst Niebur. A model of saliency-based visual attention for rapid scene analysis. *IEEE Transactions on pattern analysis and machine intelligence*, 20(11):1254–1259, 1998. 1, 2
- [19] Ming Jiang, Shengsheng Huang, Juanyong Duan, and Qi Zhao. Salicon: Saliency in context. In *2015 IEEE Conference on Computer Vision and Pattern Recognition (CVPR)*, pages 1072–1080, 2015. 2
- [20] David O Johnson and Raymond H Cuijpers. Predicting gaze direction from head pose yaw and pitch. In *2013 International Conference on Image Processing, Computer Vision, & Pattern Recognition (ICCV 2013)*, pages 662–668. World Academy Of Science, 2013. 5
- [21] Tilke Judd, Krista Ehinger, Frédo Durand, and Antonio Torralba. Learning to predict where humans look. In *2009 IEEE 12th international conference on computer vision*, pages 2106–2113. IEEE, 2009. 2
- [22] Petr Kellnhofer, Adria Recasens, Simon Stent, Wojciech Matusik, and Antonio Torralba. Gaze360: Physically unconstrained gaze estimation in the wild. In *Proceedings of the IEEE/CVF international conference on computer vision*, pages 6912–6921, 2019. 2
- [23] Christof Koch and Shimon Ullman. Shifts in selective visual attention: towards the underlying neural circuitry. In *Matters of intelligence: Conceptual structures in cognitive neuroscience*, pages 115–141. Springer, 1987. 2
- [24] Kyle Krafka, Aditya Khosla, Petr Kellnhofer, Harini Kannan, Suchendra Bhandarkar, Wojciech Matusik, and Antonio Torralba. Eye tracking for everyone. In *Proceedings of the IEEE conference on computer vision and pattern recognition*, pages 2176–2184, 2016. 2
- [25] Srinivas SS Kruthiventi, Kumar Ayush, and R Venkatesh Babu. Deepfix: A fully convolutional neural network for predicting human eye fixations. *IEEE Transactions on Image Processing*, 26(9):4446–4456, 2017. 2
- [26] Matthias Kümmeler, Lucas Theis, and Matthias Bethge. Deep gaze i: Boosting saliency prediction with feature maps trained on imagenet. *arXiv preprint arXiv:1411.1045*, 2014. 1, 2
- [27] Matthias Kümmeler, Thomas SA Wallis, and Matthias Bethge. Deepgaze ii: Reading fixations from deep features trained on object recognition. *arXiv preprint arXiv:1610.01563*, 2016. 1, 2, 3

- [28] Matthias Kummerer, Thomas SA Wallis, Leon A Gatys, and Matthias Bethge. Understanding low-and high-level contributions to fixation prediction. In *Proceedings of the IEEE international conference on computer vision*, pages 4789–4798, 2017. 2
- [29] Matthias Kummerer, Thomas S. A. Wallis, and Matthias Bethge. Saliency benchmarking made easy separating models, maps and metrics. In *Computer Vision – ECCV 2018*, pages 798–814. Springer International Publishing, 2018. 2, 4
- [30] Matthias Kümmerer, Matthias Bethge, and Thomas SA Wallis. Deepgaze iii: Modeling free-viewing human scanpaths with deep learning. *Journal of Vision*, 22(5):7–7, 2022. 1, 2
- [31] Bolin Lai, Miao Liu, Fiona Ryan, and James M Rehg. In the eye of transformer: Global–local correlation for egocentric gaze estimation and beyond. *International Journal of Computer Vision*, pages 1–18, 2023. 1, 2
- [32] Guillaume Lavoué, Frédéric Cordier, Hyewon Seo, and Mohamed-Chaker Larabi. Visual attention for rendered 3d shapes. *Computer Graphics Forum*, 37(2):191–203, 2018. 1, 2
- [33] Chang Ha Lee, Amitabh Varshney, and David W Jacobs. Mesh saliency. In *ACM SIGGRAPH 2005 Papers*, pages 659–666. ACM, 2005. 1, 2
- [34] Guanbin Li and Yizhou Yu. Visual saliency based on multi-scale deep features. In *2015 IEEE Conference on Computer Vision and Pattern Recognition (CVPR)*, pages 5455–5463, Los Alamitos, CA, USA, 2015. IEEE Computer Society. 2
- [35] Yin Li, Alireza Fathi, and James M. Rehg. Learning to predict gaze in egocentric video. In *Proceedings of the IEEE International Conference on Computer Vision (ICCV)*, 2013. 1
- [36] Akis Linardos, Matthias Kümmerer, Ori Press, and Matthias Bethge. Deepgaze iie: Calibrated prediction in and out-of-domain for state-of-the-art saliency modeling. In *Proceedings of the IEEE/CVF International Conference on Computer Vision*, pages 12919–12928, 2021. 1, 2, 3
- [37] Jianxun Lou, Hanhe Lin, David Marshall, Dietmar Sauppe, and Hantao Liu. TranSalNet: Towards perceptually relevant visual saliency prediction. *Neurocomputing*, 494:455–467, 2022. 2, 4
- [38] Jeff J MacInnes, Shariq Iqbal, John Pearson, and Elizabeth N Johnson. Wearable eye-tracking for research: Automated dynamic gaze mapping and accuracy/precision comparisons across devices. *BioRxiv*, page 299925, 2018. 2
- [39] Daniel Martin, Andres Fandos, Belen Masia, and Ana Serrano. Sal3d: a model for saliency prediction in 3d meshes. *Vis. Comput.*, 40(11):7761–7771, 2024. 1, 2
- [40] Serena Mastria, Vera Ferrari, and Maurizio Codispoti. Emotional picture perception: repetition effects in free-viewing and during an explicit categorization task. *Frontiers in psychology*, 8:1001, 2017. 1
- [41] Michael Maurus, Jan Hendrik Hammer, and Jürgen Beyerer. Realistic heatmap visualization for interactive analysis of 3d gaze data. In *Proceedings of the Symposium on Eye Tracking Research and Applications*, pages 295–298, 2014. 2
- [42] Ben Mildenhall, Pratul P Srinivasan, Matthew Tancik, Jonathan T Barron, Ravi Ramamoorthi, and Ren Ng. NeRF: Representing scenes as neural radiance fields for view synthesis. *Communications of the ACM*, 65(1):99–106, 2021. 1, 3, 5
- [43] Thomas Müller, Alex Evans, Christoph Schied, and Alexander Keller. Instant neural graphics primitives with a multiresolution hash encoding. *ACM Trans. Graph.*, 41(4):102:1–102:15, 2022. 1, 2, 5, 6
- [44] Si-Ahmed Naas, Xiaolan Jiang, Stephan Sigg, and Yusheng Ji. Functional gaze prediction in egocentric video. In *Proceedings of the 18th International Conference on Advances in Mobile Computing & Multimedia*, pages 40–47, 2020. 2
- [45] Soma Nonaka, Shohei Nobuhara, and Ko Nishino. Dynamic 3d gaze from afar: Deep gaze estimation from temporal eye-head-body coordination. In *Proceedings of the IEEE/CVF Conference on Computer Vision and Pattern Recognition*, pages 2192–2201, 2022. 2
- [46] A. et. al. Paszke. Pytorch: An imperative style, high-performance deep learning library. In *Proceedings of the 33rd International Conference on Neural Information Processing Systems*, Red Hook, NY, USA, 2019. Curran Associates Inc. 5
- [47] Tim J Smith and Parag K Mital. Attentional synchrony and the influence of viewing task on gaze behavior in static and dynamic scenes. *Journal of vision*, 13(8):16–16, 2013. 1
- [48] Ran Song, Yonghuai Liu, and Paul Rosin. Mesh saliency via weakly supervised classification-for-saliency cnn. *IEEE Transactions on Visualization and Computer Graphics*, PP: 1–1, 2019. 1, 2
- [49] Ran Song, Wei Zhang, Yitian Zhao, Yonghuai Liu, and Paul L Rosin. 3D visual saliency: An independent perceptual measure or a derivative of 2d image saliency? *IEEE Transactions on Pattern Analysis and Machine Intelligence*, 45(11):13083–13099, 2023. 2
- [50] Hamed Rezazadegan Tavakoli, Esa Rahtu, Juho Kannala, and Ali Borji. Digging deeper into egocentric gaze prediction. In *2019 IEEE Winter Conference on Applications of Computer Vision (WACV)*, pages 273–282. IEEE, 2019. 2
- [51] Sanket Kumar Thakur, Cigdem Beyan, Pietro Morerio, and Alessio Del Bue. Predicting gaze from egocentric social interaction videos and imu data. In *Proceedings of the 2021 International Conference on Multimodal Interaction*, pages 717–722, 2021. 2
- [52] Eleonora Vig, Michael Dorr, and David Cox. Large-scale optimization of hierarchical features for saliency prediction in natural images. In *Proceedings of the IEEE conference on computer vision and pattern recognition*, pages 2798–2805, 2014. 2
- [53] Haofei Wang, Jimin Pi, Tong Qin, Shaojie Shen, and Bertram E Shi. Slam-based localization of 3d gaze using a mobile eye tracker. In *Proceedings of the 2018 ACM symposium on eye tracking research & applications*, pages 1–5, 2018. 2
- [54] Yinan Wang, Sansitha Panchadsaram, Rezvan Sherkaty, and James J. Clark. An egocentric video and eye-tracking dataset for visual search in convenience stores. *Computer Vision and Image Understanding*, 248:104129, 2024. 1, 5
- [55] Jiale Xu, Weihao Cheng, Yiming Gao, Xintao Wang, Shenghua Gao, and Ying Shan. Instantmesh: Efficient 3d

- mesh generation from a single image with sparse-view large reconstruction models. *arXiv preprint arXiv:2404.07191*, 2024. [1](#)
- [56] Bincheng Yang and Hongwei Li. A visual attention model based on eye tracking in 3d scene maps. *ISPRS International Journal of Geo-Information*, 10(10):664, 2021. [2](#)
- [57] Zhefan Ye, Yin Li, Alireza Fathi, Yi Han, Agata Rozga, Gregory D Abowd, and James M Rehg. Detecting eye contact using wearable eye-tracking glasses. In *Proceedings of the 2012 ACM conference on ubiquitous computing*, pages 699–704, 2012. [2](#)
- [58] Yu-Jie Yuan, Yang-Tian Sun, Yu-Kun Lai, Yuewen Ma, Rongfei Jia, and Lin Gao. Nerf-editing: geometry editing of neural radiance fields. In *Proceedings of the IEEE/CVF Conference on Computer Vision and Pattern Recognition*, pages 18353–18364, 2022. [2](#)
- [59] Jianming Zhang and Stan Sclaroff. Saliency detection: A boolean map approach. In *Proceedings of the IEEE international conference on computer vision*, pages 153–160, 2013. [2](#)
- [60] Lingyun Zhang, Matthew H Tong, Tim K Marks, Honghao Shan, and Garrison W Cottrell. Sun: A bayesian framework for saliency using natural statistics. *Journal of vision*, 8(7): 32–32, 2008. [2](#)
- [61] Mengmi Zhang, Keng Teck Ma, Joo Hwee Lim, Qi Zhao, and Jiashi Feng. Deep future gaze: Gaze anticipation on egocentric videos using adversarial networks. In *Proceedings of the IEEE conference on computer vision and pattern recognition*, pages 4372–4381, 2017. [1](#), [2](#)